Journal of Applied Polymer Science

Pre-dispersing of montmorillonite nanofiller: Impact on morphology and performance of melt compounded ethyl vinyl acetate nanocomposites

Azlin Fazlina Osman,[1] Hussein Kalo,[2] Mohd Saifullah Hassan,[1] Tew Wei Hong,[1] Farehah Azmi[1]

[1]Center of Excellence Geopolymer and Green Technology (CEGeoGTech), School of Materials Engineering, Universiti Malaysia Perlis, Arau, Perlis 02600, Malaysia

[2]Department of Inorganic Chemistry 1, University of Bayreuth, Bayreuth 95440, Germany

Correspondence: A. F. Osman (E-mail: azlin@unimap.edu.my)

ABSTRACT: Ethyl vinyl acetate (EVA) copolymers are potential materials for biomedical applications due to their exceptional mechanical properties and biocompatibility. As new medical device designs continue to reduce in size, new materials are required that exhibit improved strength and toughness. In this research, EVA nanocomposites containing synthetic montmorillonite (MMT) are being investigated as new biomedical materials with similar flexibility, biocompatibility, and biostability to neat EVA, but with far superior tensile strength and toughness. We show that the pre-dispersing of the organo-MMT prior to melt compounding with the EVA matrix can facilitate nanofiller exfoliation and dispersion in the EVA, thereby enabling significant improvement of EVA nanocomposite performance when high organo-MMT loading (5 wt %) was added. It was observed that the polarity of pre-dispersing medium influenced the nanofiller's surfactant organization and distribution, organo-MMT exfoliation, and dispersion in the EVA, and also interphases of the host copolymer. Consequently, changes in morphology have brought noticeable effects on the mechanical and thermal properties of the EVA. © 2015 Wiley Periodicals, Inc. J. Appl. Polym. Sci. **2016**, *133*, 43204.

KEYWORDS: biomedical applications; composites; copolymers; properties and characterization; structure–property relations

Received 20 August 2015; accepted 10 November 2015

DOI: 10.1002/app.43204

INTRODUCTION

The research on polymer-nanoclay based nanocomposites has gained momentum recently with the efforts to obtain high performance materials. The nanoclays are attracting considerable interest as nanofiller material as they can provide vastly superior reinforcement efficiency due to their high aspect ratio and a greater surface area to mass ratio. The incorporation of nanoclays into the host polymeric materials were reported to result in enhanced mechanical and barrier properties,[1–3] biostability,[4–6] biocompatibility,[4,6] thermal stability,[7,8] and flame retardancy[9,10] when compared with neat polymer.

Nanoclays in their pristine form are hydrophilic, thus incompatible with most polymers.[11] Their nanoplatelets tend to undergo face to face stacking, forming tactoids. These factors make the intimate contact between the polymer matrix and the nanoclay difficult.[1,11] The most critical issue in polymer nanocomposite containing nanoclay filler is to breakdown/exfoliate the tactoids to the scale of individual particles during the dispersing process to form "true nanocomposite." Fully exfoliated and well-dispersed nanoclay are vital to enhance the thermal, mechanical, and barrier properties of the resulting nanocomposites. Surface modification of the nanoclay with organic surfactants is the most widely applied method to render nanoclay miscible with polymer matrices, making intercalation of the polymer possible during the compounding process. Consequently, the exfoliation and dispersion of the nanoclay can be facilitated inside the host polymer.[11,12] Even though this ion exchanged method may enhance the compatibility between the clay and the polymer matrix, previous researches suggest that fully exfoliated structure is difficult to achieve, even when surface modified.[1,2,4–6] Direct melt compounding methods such as extrusion and internal mixing could not promise the production of fully exfoliated nanoclays with appreciable dispersion quality, even though the screw or mixing blade is capable to provide shear forces to break up large tactoids.[1,2,4–6] Hence, the intercalated nanocomposite system was frequently obtained rather than exfoliated structure. Previous work by Andriani *et al.* suggests that the poorly-dispersed organclays are more likely to leach out and pose safety risk as compared to the well-dispersed organoclays, due to their high tendency of forming large tactoids, which can easily phase separated from the host polymer.[4] For these reasons, there is an urgent need for further improving the processing method toward optimization of nanoclay delamination (exfoliation) and dispersion in the host

material. Vigorous stirring and adequate shear energy might be needed in order to break the tactoids and fully exfoliate this particular nanofiller for better dispersing ability inside the polymer matrix. One possible way is to create loosely packed nanoplalelets or swell nanoclay layers prior to melt compounding with the polymer. Therefore, we have postulated that pre-dispersing of the nanoclay in liquid medium prior to melt compounding with polymers may weaken the tactoid bonding and further facilitate the exfoliation and dispersion of the nanoclay during the melt compounding process. Previous researches proved that the swelling of the organoclays can be achieved by dispersing them in both polar and non-polar molecules, as their inter-galleries is sensitive to the absorption of both types of ancillary molecules.[13–15] The non-polar organic solvents such as toluene can be efficiently solubilized within the inter-galleries of the organo-MMT due its polarity matching with the organic surfactant used to surface modify the nanoclay. The polar liquid such as water can induce dipoles at the silicate surface, thereby providing driving force for the swelling process through the dipolar repulsion.[13–15] However, literatures suggest that there was no research concerning the benefits and effects of polar and non-polar pre-dispersing medium on the morphology and properties of melt compounded polymer nanocomposites thus far. Therefore, our current works intend to investigate the effectiveness of this pre-dispersing technique in enhancing the exfoliation and dispersion ability of the organoclay filler in the polymer matrix by specifically comparing the effects of both polarity different swelling mediums on the morphology and properties of the resulting nanocomposites.

In this research, ethylene vinyl acetate copolymer (EVA) was used as the matrix material. EVA copolymer is produced from ethylene (non-polar) and vinyl acetate (VA) (polar) monomers. EVA copolymers with different acetate contents are extensively used in many fields such as packaging, cable insulation, and biomedical industry.[16] The main advantage of EVA copolymers is their wide range of properties that can be obtained by varying the VA content. Thus, it is possible to extent the applications from rigid plastic to rubberlike/elastic products. Furthermore, EVA can be easily processed and molded by industrial methods such as extrusion, injection, blow molding, calendaring, and rotational molding.[16,17] Our recent publication indicates the potential of this particular EVA plastic for implantable devices due to enhanced biostability and biocompatibility upon the incorporation of organically modified montmorillonite (organo-MMT).[6] In this present work, EVA/organo-MMT nanocomposites were produced by pre-dispersing the organo-MMT in two types of liquid medium which were distilled water (polar) and toluene (non-polar), and followed by melt compounding with the EVA copolymer by twin-screw extruder. This melt compounding method was chosen for its suitability in manufacturing industrial-scale products. However, this current processing route offers advantages over the previously applied direct melt compounding method[6] by way of enhancing the filler exfoliation and dispersion inside the EVA matrix, thereby enabling the improvement of EVA nanocomposite performance when high organo-MMT loading (5 wt %) was added. In this article, we describe the effects of these pre-dispersing medium on the morphology, mechanical, and thermal properties of the EVA nanocomposites and communicate the benefits of this pre-dispersed organo-MMT in enhancing toughness and thermal properties of the EVA.

EXPERIMENTAL

Materials

The main raw materials used in this study were the same as previously described in our previous publication.[6] EVA copolymer (UBE EVA V215) containing 85% ethylene and 15% VA from UBE-Maruzen Polyethylene Co. Ltd., Tokyo, Japan was used as matrix material. Organically modified montmorillonite (organo-MMT), which contains 35–45 wt % dimethyl dialkyl (C14–C18) amine as an organic surfactant was used as nanofiller. This organo-MMT is commercially known as Nanomer (types 1.44P) by Nanocor, Inc. The surface modification process involves the non-stoichiometric ion exchange of the natural MMT with the amphiphilic compound (dimethyl dialkyl (C14–C18) amine) comprising the long alkyl chains. This renders the pristine hydrophilic MMT hydrophobic, thus allowing it to interface with the hydrophobic polyolefin matrices, including EVA copolymer. This beige color organo-MMT powder with chemical formula of $(Na,Ca)_{0.33}(Al,Mg)_2(Si_4O_{10})(OH)_2 \cdot nH_2O$ was supplied by Sigma-Aldrich (USA). The average particle size of this organo-clay is ≤ 20 microns, while the bulk density ranges from 200 to 500 kg/m^3. Distilled water and toluene (ACS, ISO, Reag.PhEur grade) from Merck Pty Ltd. were used as pre-dispersing medium to allow swelling of the organo-MMT.

Samples Preparation

The organo-MMTs were pre-dispersed in two types of liquid media, which were; distilled water and toluene, in order to allow swelling of nanoplatelets prior to melt compounding with the EVA matrix. These organoclays were prepared as 50 wt % solution in toluene and water respectively and the suspension was stirred at room temperature until homogenously dispersed using magnetic stirrer. The suspension using water as medium was placed in an oven at temperature of 50°C until fully dried. Based on weight observation, the organo-MMT took around 48 h to fully dry. The suspension using toluene as medium formed gel-like mixture after few hours of stirring and it was placed under the fumehood for 24 h to allow for toluene evaporation. After that, the organo-MMT was placed in the circulated oven at temperature of 50°C for another 24 h to ensure that the solvent was fully evaporated. Lastly, both water and toluene dispersed organo-MMTs were grinded and sieved to diminish agglomeration.

The EVA and organo-MMT were dried inside an oven at temperature of 50°C overnight to remove the water content prior to melt compounding with the organo-MMT. This is to ensure that melt mixing process between EVA and organo-MMT in the extruder can be optimized without the interference of moisture that can reduce the quality of the extrudate. The nanocomposite samples were prepared by melt mixing EVA copolymer with different ratios of organo-MMT filler (0, 1, 3, 5, and 7 wt %) using twin screw extruder, Lab Tech Co. (LZ80). Processing temperature used was 160°C with 150 rpm screw speed and 15 rpm feeder screw speed. Melt pressure was observed along the processing to identify any blockage in the screw barrels. The

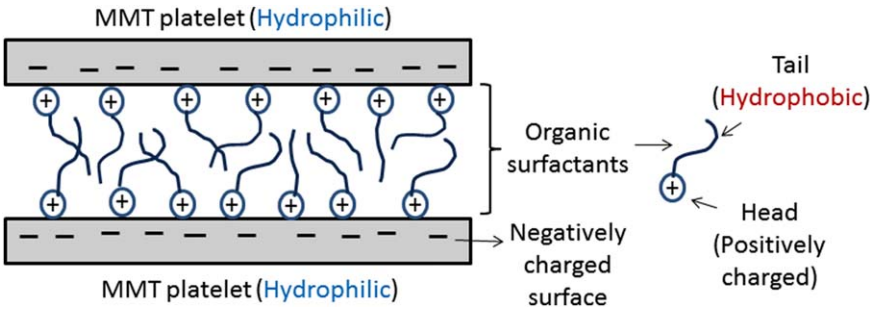

Figure 1. Basic structure of the organo-MMT nanofiller. [Color figure can be viewed in the online issue, which is available at wileyonlinelibrary.com.]

produced nanocomposites in pellet form were then compressed into 1 mm thick sheets using the compression molding machine model GT-7014-H30C from GOTECH Co. The applied hot press temperature was 160°C with 3 min of pre-heat, 4 min of pressing, and 2 min of cooling time. The specimens were cut accordingly for testing and characterization.

In the subsequent discussion, the EVA nanocomposites are referred to as EVA_XMMT (W) and EVA_XMMT (T). A number quotes as "X" denotes the weight percentage of organo-MMT loading in the EVA. The acronym "MMT (W)" represents the organo-MMT which was pre-dispersed by water medium, while the acronym 'MMT (T)' refers to the organo-MMT which was pre-dispersed using toluene medium.

Characterization and Mechanical Testing

X-ray Diffraction Analysis. X-ray diffraction (XRD) analysis on the organo-MMT nanofiller and nanocomposites was done using XRD device model Phaser-D2 manufactured by Bruker company, to characterize basal plane spacing changes in the organo-MMT, due to insertion of EVA molecular chains between the layered structure.

Transmission Electron Microscopy. The dispersion of the organo-MMT inside the EVA matrix was characterized using transmission electron microscopy (TEM). Thin sections of ~30–50 nm thickness were cut using a Diatome diamond knife on a Leica Ultracut microtome (Leica Biosystems GmbH) and placed on carbon copper grids. Samples were examined at low magnification (×12,000) and high magnifications (×93,000) on a LEO 922 A EFTEM (Carl Zeiss AG) operating at 200 kV accelaration voltage.

Fourier Transform Infrared Spectroscopy. Perkin Elmer Paragon 1000 Fourier transform infrared (FTIR) spectrometer with attenuated Total Reflectance (ATR) method was used to characterize chemical functional groups of the organo-MMT and nanocomposite samples. The samples were recorded with 32 scans in the frequency range 4000–650 cm^{-1} with a resolution of 4 cm^{-1}.

Tensile Test. The tensile test on the neat EVA and EVA nanocomposites were performed using Instron machine model-5582, according to ASTM D638 method. Five replicates of dumbbell sample from each material were tested and the testing was carried out using crosshead speed of 50 mm/min for rigid and semi-rigid material. Mean values for tensile strength and tensile toughness were taken for comparison between materials.

Thermogravimetric Analysis. Thermogravimetric analysis (TGA) on the neat EVA and EVA nanocomposites was performed using TGA Pyris Diamond PerkinElmer equipment. The weight loss of specimen against temperature was measured from 30°C to 700°C with a constant heating rate of 10°C/min, under nitrogen atmosphere.

Dynamic Thermal Mechanical Analysis. Dynamic thermal mechanical analysis (DMTA) machine from Perkin Elmer Instruments was employed to determine the thermomechanical properties of neat EVA and EVA nanocomposites. Analysis was performed at 0.1% strain in bending mode using a frequency of 1 Hz and a heating rate of 2°C/min from room temperature to 90°C.

Differential Scanning Calorimetry. Differential scanning calorimetry (DSC) measurements on the neat EVA and EVA nanocomposites were carried out using DSC Q10 analyzer (Research Instrument). The sample with the approximate weight of ~6 mg was placed in closed aluminum pan and analyzed by heating from ~35 to 130°C under nitrogen atmosphere. The heating rate employed was 10°C/min.

RESULTS AND DISCUSSION

The morphology and performance of the EVA nanocomposites containing organo-MMT prepared by direct melt compounding method (without pre-dispersing) were discussed thoroughly in our previous publication.[6] Therefore, this article focuses on the morphological data and properties of the neat EVA and EVA nanocomposites containing pre-dispersed organo-MMT. To begin the discussion, a brief description on the structure of the organo-MMT is provided and illustrated in Figure 1. It shows the interactions between the organic surfactant (dimethyl dialkyl (C14–C18) amine) with the nanoplatelets of the MMT; where both possess different polarity. The positively-charged head group of the organic surfactant is attached on the negatively-charged MMT platelet surface due to a strong electrostatic interaction.[18] Given that the EVA copolymer also comprised of the hydrophobic polyethylene (PE) and hydrophilic (PVA) molecular chains, the presence of the organo-MMT in the polymer structure would result in polar and non-polar interactions between these components. The pre-dispersing of the organo-MMT in the hydrophilic (water) and hydrophobic (toluene) medium would also affect the distribution and arrangement of the MMT nanoplatelets and the organic surfactant, and hence their interactions with the host polymer. The

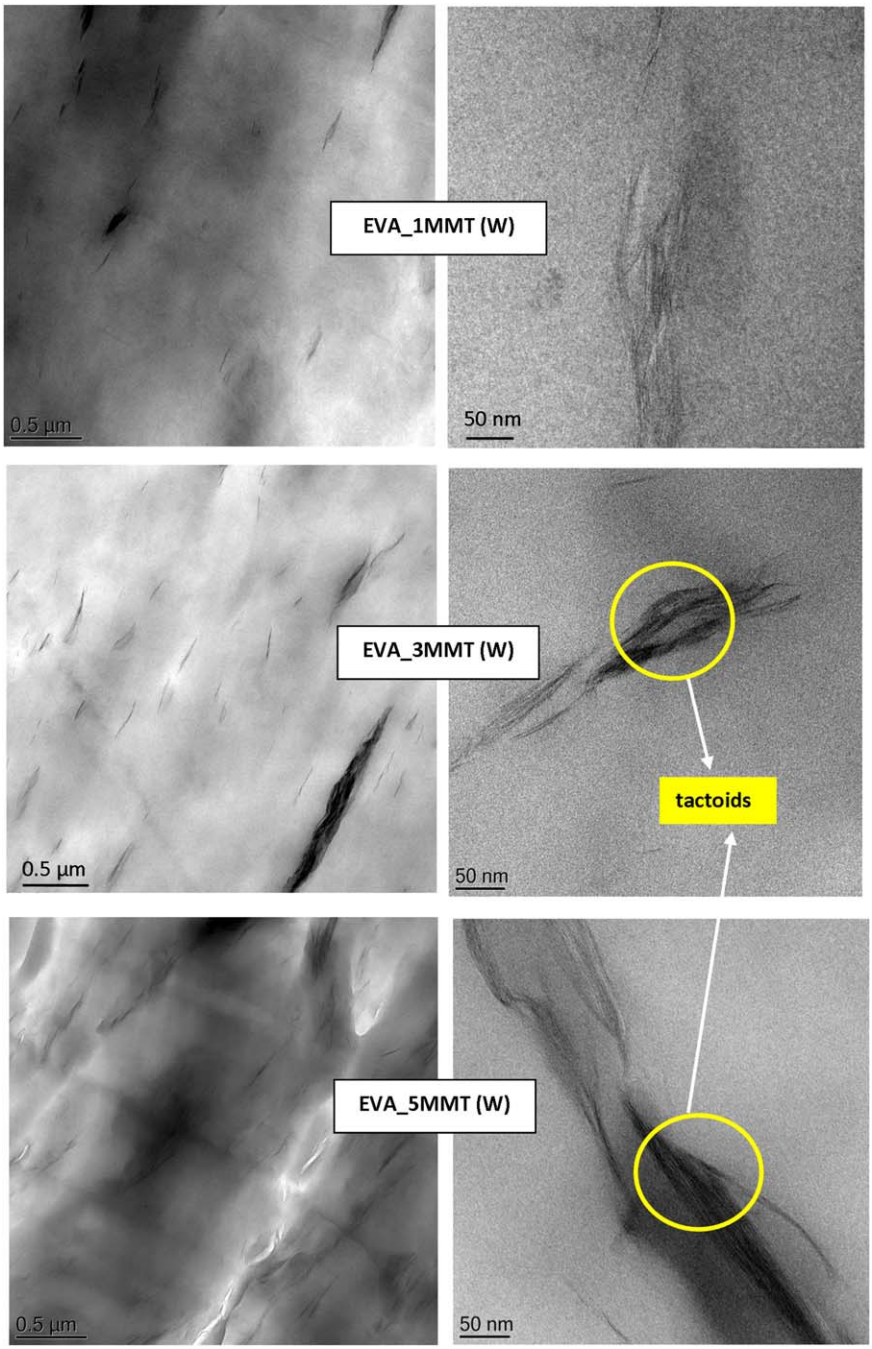

Figure 2. TEM micrographs of EVA nanocomposites containing water dispersed organo-MMT with different nanofiller loadings. [Color figure can be viewed in the online issue, which is available at wileyonlinelibrary.com.]

understanding of these polar and non-polar interactions between the organo-MMT, the host EVA copolymer, and pre-dispersing mediums is an important focal point of this article. Therefore, the following discussion focuses on the relationships between these aspects with the properties of the obtained EVA nanocomposites.

TEM Analysis of the EVA Nanocomposites (Dispersity Analysis)

The effect of pre-dispersing medium on the morphology of EVA nanocomposites containing organo-MMT was investigated by TEM analysis. TEM images of the EVA nanocomposites containing pre-dispersed organo-MMT by water and toluene medium are shown in Figures 2 and 3, respectively.

Generally, the quality of organo-MMT dispersion and distribution in the EVA matrix was slightly reduced as the nanofiller loading increased from 1 to 5 wt %. This was due to the collision between the nanoclay platelets that increase with the concentration, thus leading to agglomeration and greater spatial restriction for the tactoid delamination.[6,19] The EVA nanocomposites exhibit a mixed morphology of exfoliated or intercalated structure, in which the size of stacking platelets (tactoid) was

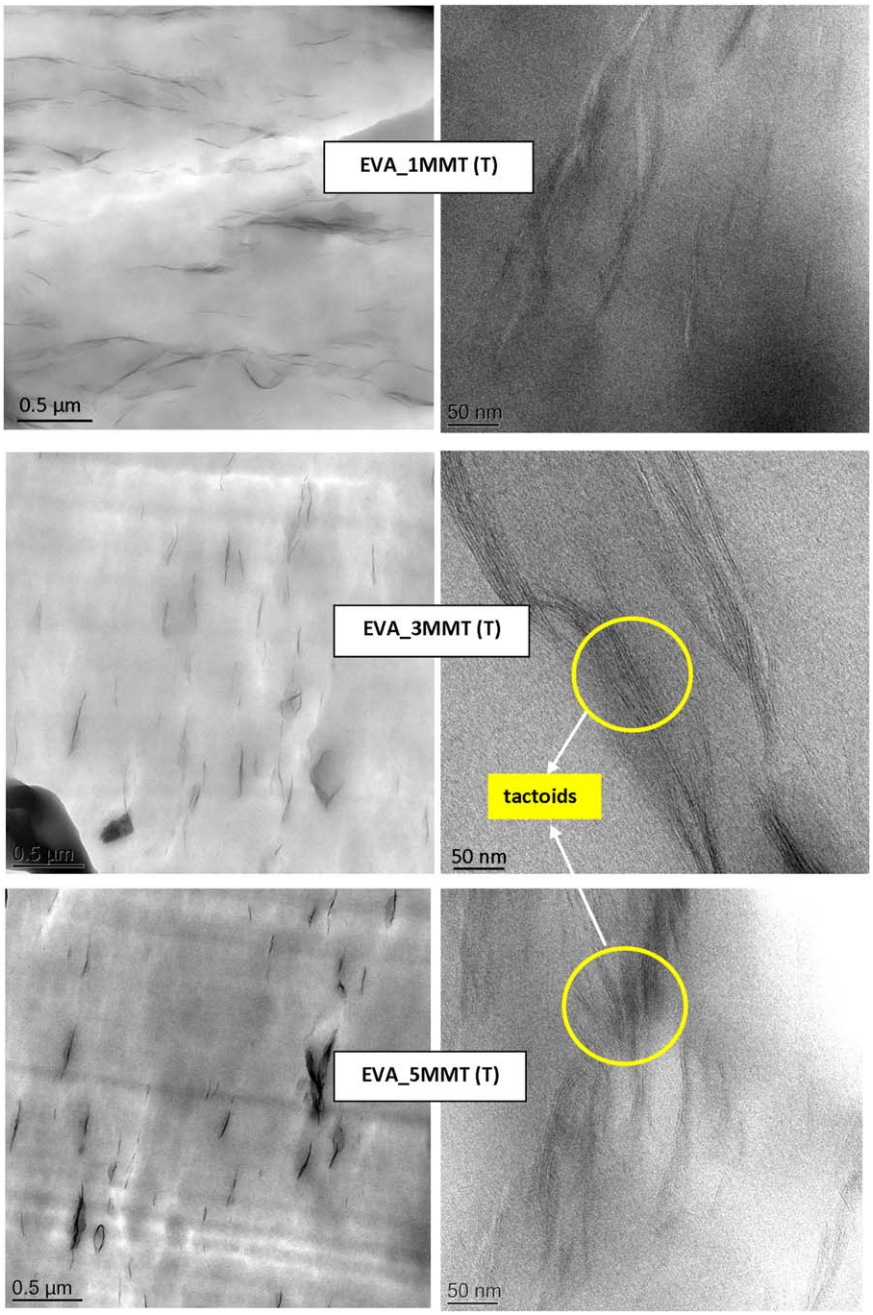

Figure 3. TEM micrographs of EVA nanocomposites containing toluene dispersed organo-MMT with different nanofiller loadings. [Color figure can be viewed in the online issue, which is available at wileyonlinelibrary.com.]

larger for the nanocomposite system containing water dispersed organo-MMT [EVA_XMMT (W)]. At the same nanofiller loading, the degree of exfoliation and dispersion of the organo-MMT dispersed by toluene were greater as compared to the water dispersed counterpart. The similar EVA-MMT nanocomposite system has been studied and reported in our recent publication.[6] In contrast with this current work, there was no pre-dispersing technique applied prior to melt compounding with the EVA. Therefore, larger organo-MMT tactoids was found in the nanocomposite sample containing high loading (5 wt %) organo-MMT (see Figure 4).

This suggests that the pre-dispersing technique can facilitate the dispersion of the nanofiller, and toluene is a better dispersing medium than water to enhance the dispersion and exfoliation quality of the organo-MMT throughout the EVA matrix. As the non-pre-dispersed organo-MMTs tend to arrange in face-to-face stacking, insufficient shear energy may result in poor delamination efficiency, thus making more difficult for the polymer to intercalate them into single layers (exfoliated structure). The shear energy provided by the twin screw extruder during the compounding with the polymer may not be enough to produce fully exfoliated organo-MMT structure, especially when the

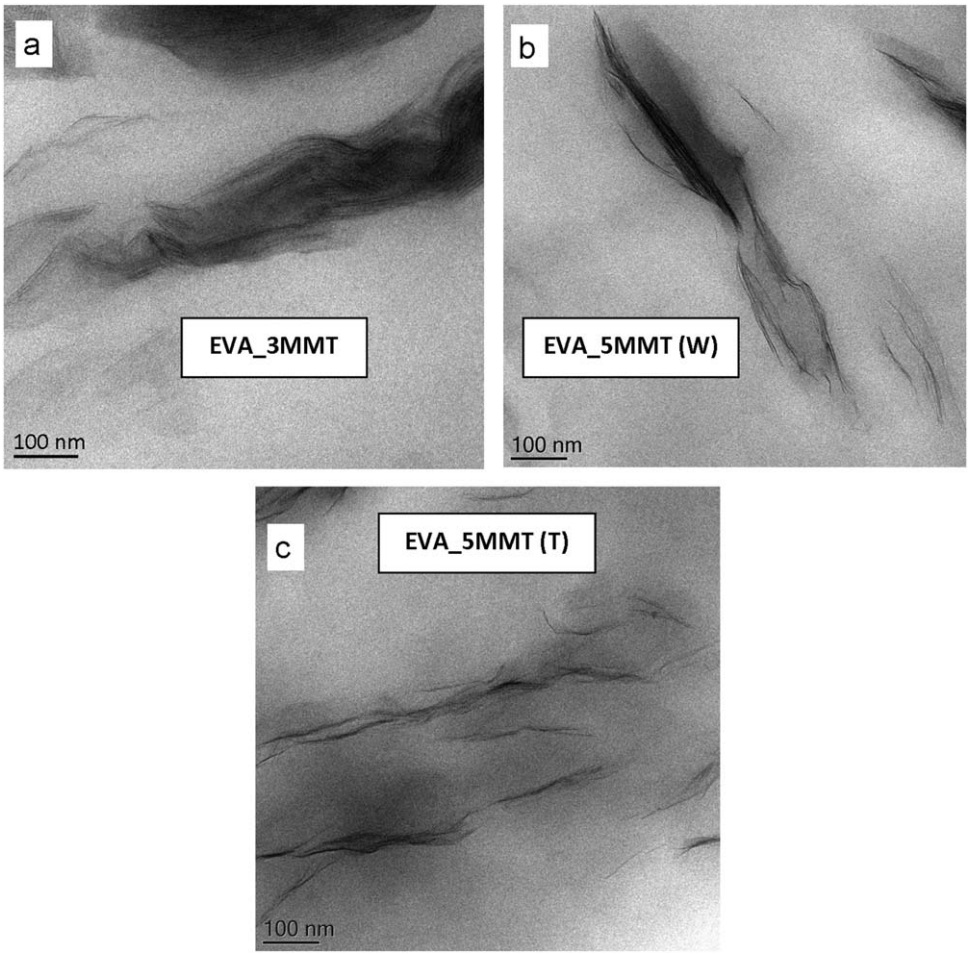

Figure 4. TEM images of the EVA nanocomposites incorporating 5 wt % organo-MMT, in which the nanofiller were (a) not pre-dispersed, (b) pre-dispersed by water (MMT (W)), (c) pre-dispersed by toluene (MMT (T)). The smallest tactoid size can be seen in the (c) image, due to the application of pre-dispersing technique and toluene as medium.

nanofiller loading is greater than 2 wt %. This was proved by several studies.[1–6] Therefore, this project has introduced the pre-dispersing technique to increase the organo-MMT exfoliation efficiency prior to melt compounding with the EVA. The results have successfully provided evidence that this pre-dispersing technique can contribute to enhance exfoliation capability of this nanofiller, where the toluene appears to be a better dispersing medium than water.

XRD Analysis on the Organo-MMT, Neat EVA, and EVA Nanocomposites

The XRD pattern of the nanofiller (pre-dispersed organo-MMTs (MMT (W) and MMT (T)), neat EVA, and EVA nanocomposites is presented in Figure 5. Table I summarizes the basal spacings of the MMT (W) and MMT (T) nanofillers and their respective nanocomposites, which were determined from the peak position. Basal spacings were determined using Bragg's Law ($n\,n\lambda = 2d\sin\theta$).

The results reveal the influence of nanofiller pre-dispersing medium and loading on swelling and exfoliation degree of the organo-MMT in the host EVA. Similar to our previous finding, the XRD profile of the neat EVA does not show any diffraction peaks between $2\theta = 0.5°$ to $10°$.[6] MMT (W) and MMT (T) nanofillers exhibit similar XRD signature, where d_{001} and d_{002} basal spacings of 2.7 nm and 1.3 nm appear in the 2theta range of 1–10°. The values are similar to the non-pre-dispersed

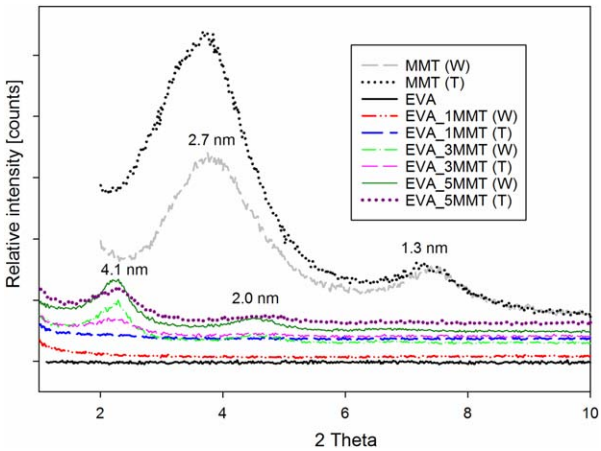

Figure 5. XRD pattern of organo-MMT pre-dispersed by water (MMT (W) and toluene (MMT (T)), before and after being incorporated into the host EVA. [Color figure can be viewed in the online issue, which is available at wileyonlinelibrary.com.]

Table I. Basal Spacings of Nanofillers, Neat EVA and EVA Nanocomposites as Obtained from XRD

	Basal spacing (nm)	
Material	d_{001}	d_{002}
MMT (W)	2.7	1.3
MMT (T)	2.7	1.3
EVA	-	-
EVA_1MMT (W)	-	-
EVA_1MMT (T)	-	-
EVA_3MMT (W)	4.1	-
EVA_3MMT (T)	4.1	-
EVA_5MMT (W)	3.9	2.0
EVA_5MMT (T)	3.9	-

organo-MMT,[6] suggesting that the pre-dispersing of the organo-MMT using both distilled water and toluene did not result in the expanding of basal spacing. Since the pre-dispersed organo-MMTs were fully dried prior to further processing/testing, their basal spacings were expected to return to the origin state (as before pre-disperse). However, when the pre-dispersed MMT was incorporated into the EVA, the crystalline peaks caused by the stacking of the nanoclay platelets were either moved to smaller angles, showing an increase in spacing or disappearing completely due to the intercalation of the host polymer. As compared to the EVA nanocomposites containing non-predispersed organo-MMT,[6] the EVA_XMMT (W) and EVA_XMMT (T) nanocomposites possess less intense diffraction signatures with lesser number of well-defined peaks, suggesting that the applied pre-dispersing technique may result in more significant reduction of the nanoplatelets long-range order with more disruption in the organo-MMT layer arrangement/stacking in the EVA. With regards to this factor, it was postulated that upon the pre-dispersing process, the organo-MMT powder was in the form of loosely packed tactoids (destabilized condition) rather than swelling. However, the incorporation of these destabilized organo-MMTs into the EVA was believed to cause higher tendency of exfoliation process to take place, due to weaker tactoid/inter-platelets bonding. Therefore, this particular pre-dispersed organo-MMT tends to disperse more easily throughout the EVA matrix. This finding again supports the hypothesis that the pre-dispersing of the organo-MMT prior to melt compounding with the EVA can enhance the quality of intercalation/exfoliation and dispersion of the EVA nanocomposites. In agreement with TEM analysis, the XRD pattern of the EVA nanocomposites suggests the reduced quality of organo-MMT exfoliation and dispersion in EVA matrix upon an increase in nanofiller loading. XRD pattern for both EVA_1MMT (W) and EVA_1MMT (T) exhibits an amorphous halo, which could be due to either the loss of long range nanoplatelets order, or alternatively caused by the increase of basal spacing beyond that detectable by XRD. In contrast, the EVA nanocomposites containing 3 wt % MMT (W) and MMT (T) demonstrate a well-defined (d_{001}) peak centered at ~2.15°, which corresponds to a basal spacing of 4.1 nm. Further increase in nanofiller loading from 3 wt % to 5 wt % resulted in the decrease of basal spacing from 4.1 nm to 3.9 nm. Apparently, at 3 and 5 wt % nanofiller loadings, EVA_XMMT (T) nanocomposites demonstrate weaker XRD signals than EVA_XMMT (W) nanocomposites. This could be due to better EVA intercalation between the MMT (T) platelets, which produced smaller tactoids. The efficiency of EVA intercalation and organo-MMT exfoliation would depend on the destabilization effect caused by the pre-dispersing medium. It was anticipated that upon the pre-dispersing process, the organization of the hydrophobic surfactant on the clay surface would depend on the polarity of the pre-dispersing medium. This is because, the structure of the dimethyl dialkyl (C14–C18) amine organic surfactant comprises of the charged head groups that can interact with the hydrophilic clay surface and the bulky hydrocarbon tails that occupying the inter-gallery space. The lower degree of destabilization effect of the MMT in water could probably due to the hydrophobic characteristic of the dimethyl dialkyl (C14–C18) amine surfactant, which prevents organo-MMT platelet separation in hydrophilic environments. When using water medium, the surfactant's hydrophobic tails would attempt to "hide" from the hydrophilic environment, accumulate, and cause precipitation.[20,21] This might prevent the entrance of greater amounts of water molecules into the organo-MMT inter-galleries in order to destabilize the binding energy within the inter-galleries. Consequently, this could hinder larger degree of tactoid loosening during the pre-dispersing process. Due to their long segment and restricted mobility, there is also high possibility that most of the surfactant chains retain its organization and distribution in the MMT, even when the water dried off. When the MMT (W) added to the EVA matrix, the inhomogeneous surfactant distribution led to weaker nanofiller–polymer interactions and hence poorer quality of nanofiller dispersion. Furthermore, the affinity of the accumulated surfactant toward the hydrophobic PE chains also could reduce the homogeneity of the PVA and PE chains distribution in this EVA copolymer. Certainly, these would not occur when hydrophobic pre-dispersing medium (toluene) was used, as the hydrophobic surfactant would not repel toluene from entering the inter-galleries. As a result, the incorporation of MMT (T) into the EVA host polymer caused higher degree of exfoliation and dispersion as compared to MMT (W). Further evidence on this "destabilization effect" was obtained from the FTIR analysis and will be discussed later in the following section.

XRD analysis in the range of $2\theta = 12°$ to 25° was done to investigate the effects of MMT (W) and MMT (T) nanofillers on the morphology of the EVA. Based on Figure 6, the neat EVA copolymer demonstrates two well-defined peaks centered at ~21.3° and ~23.4° respectively due to crystalline structure of polyethylene (PE).[22]

When 5MMT (T) being incorporated into the host EVA, the intensity of both peaks was reduced, showing that this nanofiller has resulted in increased imperfection of existing chain crystallites. This is expected as the crystallization of the non-polar PE chains can be hindered due to hydrophobic interactions with the organo-MMT nanofiller and this effect can also been observed in the work by Merinska *et al.*[23] However, the addition of 5MMT (W) into the EVA has resulted in further reduction in the intensity of both peaks. It can be postulated that the precipitated long and hydrophobic surfactant's tails would interact more preferentially with PE chains due to their polarity matching. This interaction would bring greater

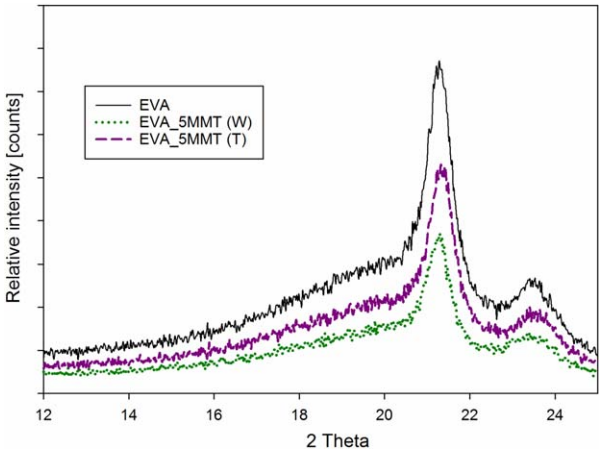

Figure 6. The effects of MMT (W) and MMT (T) nanofillers on the XRD pattern of the EVA. [Color figure can be viewed in the online issue, which is available at wileyonlinelibrary.com.]

thermodynamic barrier for nucleation process and hence, reduce the crystallinity of the PE. Therefore, less intense peaks can be observed in the EVA_5MMT (W) as compared to both neat EVA and EVA_5MMT (T).

Fourier Transform Infrared Analysis

Figure 7(a,b) presents the FTIR spectra of the organo-MMT nanofillers (pre-dispersed and without pre-dispersed) and neat EVA and EVA nanocomposites respectively.

For the non-dispersed organo-MMT sample (MMT), the peaks observed at ~1000 cm^{-1}, ~918 cm^{-1}, and 800 cm^{-1} are attributed to internal vibrations of Si—O—Si of silicate layers.[24,25] The peaks centered at ~3650 cm^{-1} and ~1646 cm^{-1} corresponded to structural O—H stretching vibration in the MMT, due to adsorbed molecules of water.[24,26] The spectra of this organo-MMT also indicate the presence of methylene groups from the grafting of organic surfactant (2850 cm^{-1} and 2912 cm^{-1}).[25] The band at ~1469 cm^{-1} is associated to the quaternary ammonium.[24] The small peaks presence at ~1120 cm^{-1} and ~919 cm^{-1} were assigned to CH_2 vibrations of the surfactant and in plane stretching vibrations of the tetrahedral silicate layers, respectively. Changes in the morphology can be detected when this organo-MMT was pre-dispersed by water and toluene. The intensity of the spectra was seen to reduce throughout all regions. The less intense spectral band observed in the region of ~750–1300 cm^{-1} arises from the weaker signal of Si—O—Si vibrations, due to the destabilization of the binding energy within the silicate inter-galleries upon the pre-dispersing process. Furthermore, MMT (T) presents the weakest FTIR signals among other nanofillers, showing that the pre-dispersing of the organo-MMT using toluene medium resulted in the greatest "destabilization effect" and weakest interlayer binding energy. The following statements provide further explanation on this phenomenon. Infrared spectroscopy analysis is basically a study of interaction of infrared light with matter. The absorption of infrared radiation by a molecule will result in its chemical bond vibration.[27] Therefore, changes in peak intensity signify changes related to the molecular bond. The organo-MMT nanoplatelets structure consists of an inner octahedral layer being sandwiched between two silicate tetrahedral layers.[13] Their inter-galleries contain the organic surfactants, which are grafted on opposite surfaces of the nanoplatelets. These inter-galleries are being referred to as "organic layers" in this discussion. During the pre-dispersing process, the solvents (water and toluene) may enter the "organic layers" of the MMT structure and occupy the free spacing between the organic surfactants. This "solvation power" caused the swelling of the "organic layer," disrupt the MMT layer lattice and destabilize the inter-galleries binding energy. As a result, the pre-dispersed organo-MMT exhibit weaker signals of Si—O—Si vibrations in 750–1300 cm^{-1} region, especially when non-polar toluene solvent (with greater affinity toward the organic layer) was used as pre-dispersing medium. Nevertheless, the presence of the organic surfactant can still be detected in the spectra, suggesting that the pre-dispersing process by water and toluene did not diminish the surface modification of the organo-MMT. In addition, the observed less intense ~3650 cm^{-1} and ~1646 cm^{-1} peaks suggest that the pre-dispersed MMTs absorbed less water compared to non-pre-dispersed MMT.

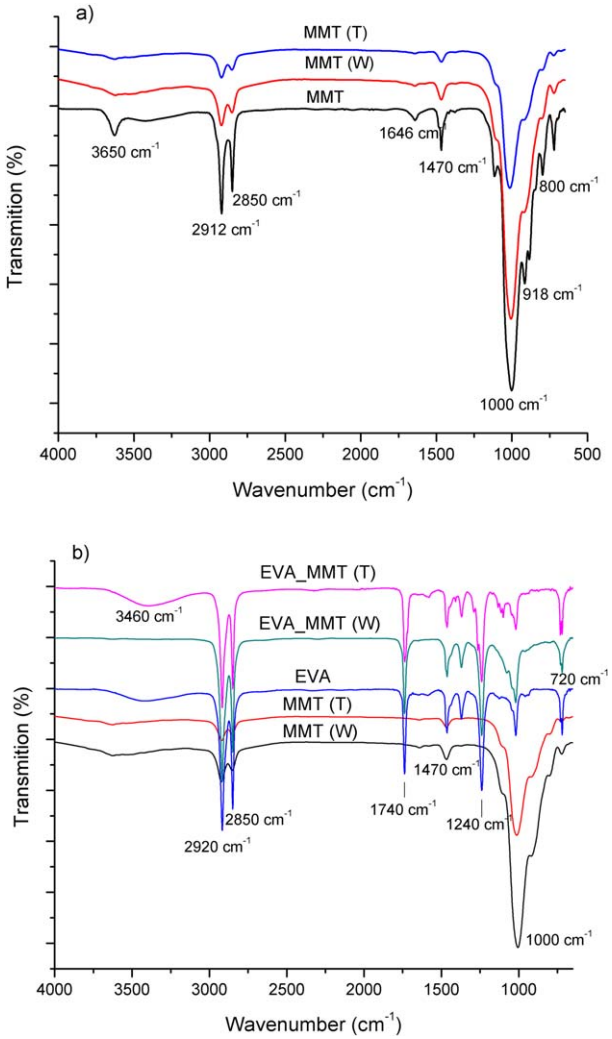

Figure 7. FTIR spectra of the (a) organo-MMT nanofillers (non-predispersed and pre-dispersed) and (b) neat EVA, EVA_5MMT (W) and EVA_5MMT (T) nanocomposites. [Color figure can be viewed in the online issue, which is available at wileyonlinelibrary.com.]

Table II. Tensile Properties of Neat EVA and EVA Nanocomposites Incorporating Water Dispersed Organo-MMT and Toluene Dispersed Organo-MMT

Mechanical properties	EVA	Pre-dispersing medium	EVA+1% MMT	EVA+3% MMT	EVA+5% MMT	EVA+7% MMT
Tensile strength (MPa)	9.1 ± 0.2	Water	9.7 ± 0.4	10.0 ± 0.1	12.9 ± 0.5	10.2 ± 0.2
		Toluene	12.9 ± 0.4	14.8 ± 0.05	17.1 ± 0.4	16.3 ± 0.2
Toughness (MPa)	43.7 ± 2.0	Water	55.7 ± 2.6	78.2 ± 1.5	80.5 ± 2.5	79.7± 1.4
		Toluene	74.2 ± 3.0	79.6 ± 1.4	86.5 ± 3.0	83.4 ± 1.3

For neat EVA, the absorbances of the polyethylene groups can be observed from the spectra peaks of ~2920 cm^{-1}, ~2850 cm^{-1}, ~1470 cm^{-1}, and ~720 cm^{-1}.[27,28] Several peaks at ~1740 cm^{-1}, ~1240 cm^{-1}, ~1020 cm^{-1}, and ~610 cm^{-1} were assigned to VA contents or units.[27,28] A shoulder around ~3460 cm^{-1} was attributed by carbonyl (C═O) overtone.[26,27] Based on FTIR pattern, the incorporation of the 5MMT (W) and 5MMT (T) into the host EVA resulted in some alterations in the EVA morphology. The FTIR spectra of both EVA nanocomposites clearly exhibit the characteristic absorptions bands that are attributable to host EVA and organo-MMT. For EVA_5MMT (T) nanocomposite sample, the intercalation of polymer chain between the layers of the organo-MMT has resulted in the appearance of new peaks in the regions of 1110 and 1590 cm^{-1} and stronger band in 3000–3645 cm^{-1} region. These bands could be derived from the bending vibrations of organo-MMT, together with the stretching of structural hydroxyl (—OH) and Si—O groups, indicating the existence of MMT (T) nanofiller in the EVA matrix.[25] The disappearance of the bands in 1590 cm^{-1} and 3000–3645 cm^{-1} region for EVA_5MMT (W) sample can be associated with weaker interaction between the 5MMT (W) and EVA, as compared to 5MMT (T) counterpart. In agreement with the TEM and XRD analyses, these weaker EVA/organo-MMT interactions resulted in reduced quality of nanofiller dispersion inside the EVA matrix (Figures 2 and 5). Furthermore, EVA_5MMT (W) sample exhibits stronger band at ~900–1000 cm^{-1} region as opposed to EVA and EVA_5MMT (T). This could be the signal of stronger silicate layer bonding in the structure of EVA_5MMT (W) nanocomposite as compared to EVA_MMT (T), due to the presence of more stable and larger tactoids. This correlates well with the previous TEM and XRD results.

Tensile Test

Tensile test was done to compare the tensile strength and toughness values of all the materials. Table II indicates the tensile properties of neat EVA and EVA nanocomposites containing organo-MMT nanofiller that have been pre-dispersed by water and toluene. Figures 8 and 9 compare the mean values of tensile strength and tensile toughness of these materials respectively.

It can be summarized that the addition of the pre-dispersed organo-MMT (by both water and toluene has brought the enhancement of tensile properties of the EVA. Generally, the increase of nanofiller loading from 0% to 5% resulted in steady increase of tensile strength and tensile toughness. However, further increase of the organo-MMT loading to 7 wt % caused reduction of these properties. Therefore, the assumption has been made that the optimum organo-MMT loading for this EVA system (using current methodologies) was 5 wt %. As the reduction in mechanical performance was not of particular interest in this study, the graphs of EVA nanocomposite containing 7 wt % were not plotted in the corresponding Figure 8 and 9, and the following parts of this paper will not discuss this system.

Apparently, the use of toluene as pre-dispersing medium for the organo-MMT nanofiller has resulted in greater mechanical performance of the EVA as compared to water medium. The highest tensile strength and toughness was achieved when the EVA was added with 5 wt % MMT (T), where those values have markedly increased by ~88% and ~91% respectively. On the other hand, when the EVA was added with 5 wt % MMT (W), the values of tensile strength and toughness were only increased by ~42% and ~84% respectively. Our previous work on the same EVA-MMT nanocomposite system reported that the addition of 5 wt %

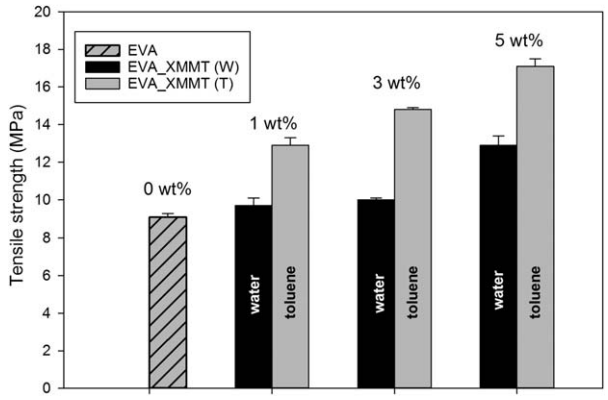

Figure 8. Tensile strength of neat EVA and EVA nanocomposites incorporating water dispersed organo-MMT and toluene dispersed organo-MMT.

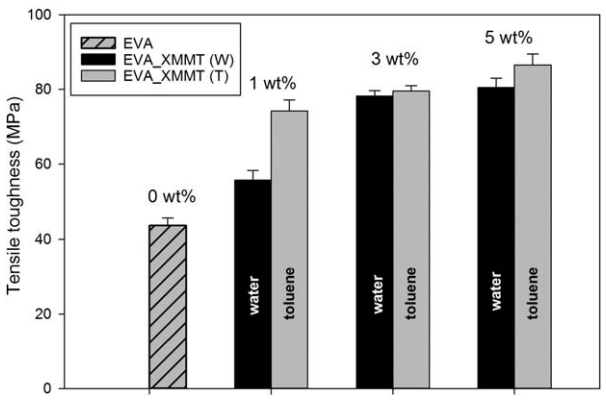

Figure 9. Tensile toughness values of neat EVA and EVA nanocomposites incorporating toluene and water dispersed organo-MMT.

Table III. Thermal Degradation Peak Temperature (T_{dmax}) of EVA and EVA Nanocomposites

Material	First step mass loss T_{dmax} (°C)	Second step mass loss T_{dmax} (°C)
EVA	368	470
EVA_5MMT (W)	335	461
EVA_5MMT (T)	350	480

organo-MMT (without pre-dispersed) has only resulted in slight increase of tensile strength and toughness, which were 2.4% and 13.6%, respectively.[6] Of particular interest, these findings are in good agreement with the TEM and XRD analyses that revealed better exfoliation and dispersion quality of organo-MMT in the EVA was obtained when this nanofiller was pre-dispersed prior to melt compounding, most significantly by using toluene (Figures 4 and 5). The greater the degree of exfoliation and dispersion, the greater the mechanical performance will be as the number of single layer of organo-MMT platelets interacting with the EVA molecular chains increases. Several researches proved that the presence of large clay tactoids may disrupt the load transfer efficiency, thus leads to the reduction of tensile strength of the host polymer.[1,2,6] In contrast, thinner and more mobile nanoplatelets can be more preferentially align in the direction of the stress, allowing the achievement of higher elongation at break and toughness.[6] This toughness property is very important to resist the material from crack propagation when subjected to high stress loading, and of course is a valuable criterion for most applications. It is quite impressive to observe the significant increment of tensile toughness upon the increase of organo-MMT loading from 0 to 5 wt %, as most of the conventional microcomposite systems show detrimental values of toughness property when the tensile strength achieved higher values upon the addition of filler. To further investigate the potential of these nanocomposites, TGA and DMTA analyses were performed to evaluate the performance of these nanocomposites under elevated temperatures.

Thermogravimetry Analysis

TGA was employed to study and compare the thermal stability of neat EVA and EVA nanocomposites with 5 wt % filler loading, pre-dispersed using water and toluene. The thermal stability in this case is based on the maximum temperature for degradation (T_{dmax}) of neat EVA and EVA nanocomposites and the rate of mass loss. Table III summarizes the thermal degradation peak temperature of all materials, while Figure 10(a,b) displays the TGA and DTG curves of the neat EVA and EVA nanocomposites respectively.

Based on Figure 10, the decomposition process of the EVA occurred in two steps, referred as first step mass loss and second step mass loss. The first mass loss step between 300 and 400°C was due to deacetylation process, which involves the releases of gaseous acetic acid and formation of C═C along the polymer backbone. The second mass loss step between 400 and 500°C was attributed to the oxidation and volatilization of hydrocarbons resulting from the decomposition of main EVA backbone.[29,30]

The T_{dmax} of the first step mass loss of EVA nanocomposites containing 5 wt % organo-MMT (water and toluene dispersed) occurred at lower temperature as compared to the neat EVA. This could probably due to the degradation of organic surfactant.[29] The degradation of dimethyl dialkyl (C14–C18) amine, that used to surface modified the MMT accelerated the degradation of PVA to acetic acid. Lower degradation temperature observed in the nanocomposite samples was due to strong catalytic effect of the organo-MMT on the deacetylation of EVA containing vinyl acetate during the decomposition process.[29,30] However, more pronounced effect can be seen in the EVA_5MMT (W) sample. It exhibits lower T_{dmax} of this first step mass loss than EVA_5MMT (T). Poorer EVA-nanofiller interactions may lead to more severe catalytic effect on the deacetylation of EVA during the decomposition process. This is because, the non-homogeneity of the organic surfactants distribution in the EVA and the subsequent weaker interactions with both MMT nanoplatetets and the EVA molecular chains provides less shielding for the degradation process of the organic surfactant. As the organic surfactant degrade faster, it will bring stronger catalytic effect to the deacetylation of the EVA. Furthermore, the inhomogeneity of the organic surfactant distribution upon the hydrophilic water medium exposure could result in weaker PE-PVA interphase bonding in this host copolymer,

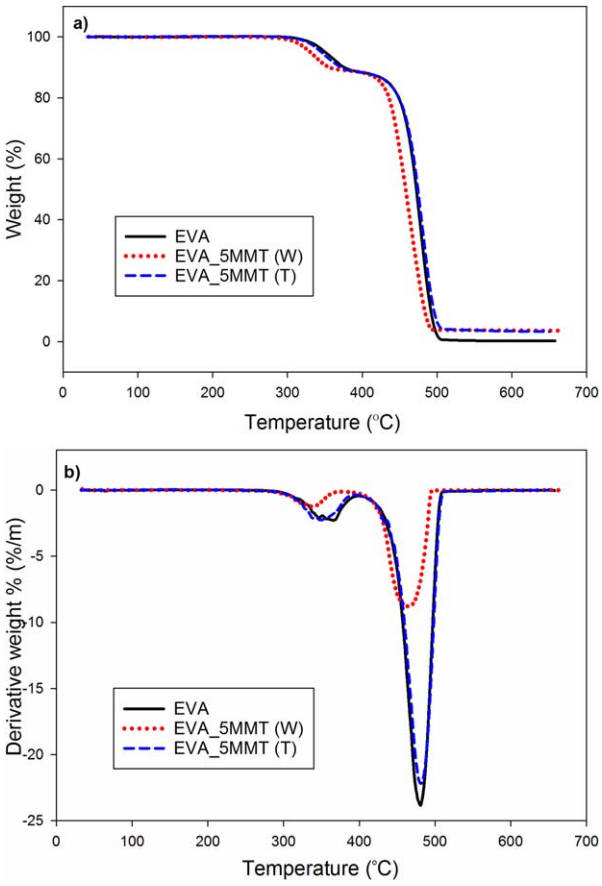

Figure 10. TGA thermograms (a) and DTG thermograms (b) of neat EVA, EVA_5MMT (W) and EVA_5MMT(T) nanocomposites. [Color figure can be viewed in the online issue, which is available at wileyonlinelibrary.com.]

Table IV. Maximum Transition Temperature Determined from DMTA

Material	T_1 (°C)	T_2 (°C)
EVA	43	-
EVA_5MMT (W)	44	60
EVA_5MMT (T)	45	-

therefore lower thermal energy was needed for deacetylation of EVA during the decomposition process.

The T_{dmax} of second step mass loss of EVA_5MMT (T) nanocomposite occurred at a higher temperature compared to the neat EVA. The layered nanoplatelets may result in more restricted polymer chain, which require higher temperature to break the molecular chains. In contrast, the nanocomposite containing 5MMT (W) resulted in the decrease of the T_{dmax} of second mass loss step of the EVA. This was possibly due to the poorer quality of organo-MMT dispersion in this sample (Figure 3) and weaker bonding between the organo-MMT and the EVA as proposed by FTIR and XRD. In Figure 9(a), the nanocomposites contributed to residues, which can be seen from ~3% remaining sample weight at ~500°C, due to the presence of the inorganic content of organo-MMT (silicate only and without organic surfactant).

The intensity of the derivative thermo gravimetric (DTG) peak (rate of mass loss) depends on the amount of degradation product releases, which is attributed to the degree of interaction between the EVA polar and nonpolar phases, and also the EVA-nanoclay interaction.[29–31] Upon the incorporation of 5 wt % MMT (T) into the EVA, lower rate of mass during the second step decomposition process [Figure 10(b)] was observed. This might be corresponded to the longer time needed to break the backbone of the copolymer, due to more restricted mobility of the EVA chain as a result of organo-MMT-EVA interactions. Other than the degree of nanofiller dispersion and exfoliation, changes in multiphase structure of the copolymer also can affect the shape/intensity of the DTG curve. For instance, lower rate of mass loss observed in the EVA_5MMT (W) sample during

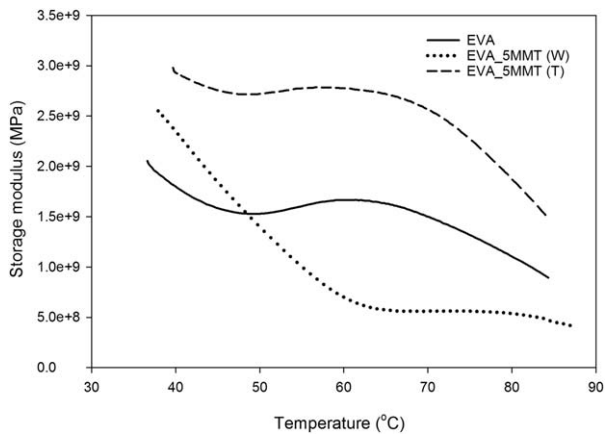

Figure 11. Storage modulus versus temperature curve of neat EVA and EVA nanocomposites incorporating water dispersed organo-MMT and toluene dispersed organo-MMT.

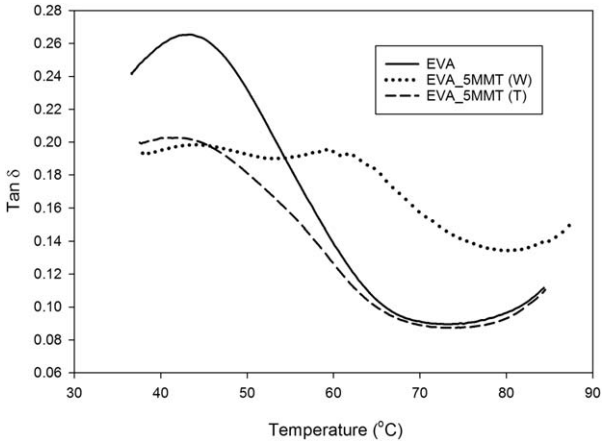

Figure 12. Tan δ versus temperature curves of neat EVA and EVA nanocomposites incorporating 5 wt % water dispersed organo-MMT (MMT (W)) and toluene dispersed organo-MMT (MMT (T)).

both mass loss steps may be associated with changes in the concentration in the melt. The EVA was believed to contain wider molar mass distribution due to the greater inhomogeneity of PE and PVA phases sequence and ordering when subjected to higher temperature. The changes in EVA morphology upon the inclusion of 5 wt % MMT (W) nanofiller were further justified using DMTA.

Dynamic Thermal Mechanical Analysis

DMTA has been increasingly used to study the relationships between the polymer structure, dispersed phase as well as the nanofiller structure in the properties of polymer nanocomposite systems.[1,2,32–35] In this study, DMTA was performed to measure the response of materials to an oscillatory deformation as a function of temperature. The results of DMTA was analyzed by considering three physical properties: (a) the storage modulus (E'), corresponding to the elastic response to the deformation, (b) the loss modulus (E''), relates to plastic response to the deformation, and (c) tan δ; the ratio of (E''/E'), a measure of the damping behavior which is useful for determining the occurrence of molecular mobility during thermal transitions.[32,33] The tan δ peaks and the peak positions are given in Table IV while the tan δ and E' curves determined by DMTA are presented in Figures 11 and 12 respectively.

Similar to previous researches, the obtained DMTA data are strongly affected by the degree of exfoliation and dispersion of the nanofiller.[1,2,32–35] When comparing the tensile test and DMTA results of neat EVA and EVA containing 5 wt % organo-MMT, one could agree that the types of pre-dispersing medium give more significant effect to the thermomechanical properties than the ambient mechanical properties of the host EVA.

Figure 11 demonstrates that the presence of the 5 wt % water dispersed organo-MMT (MMT (W)) into the EVA resulted in the enhancement in storage modulus in the 40–50°C region, followed by significant reduction in storage modulus at higher temperature region (50–85°C). During this high temperature region (rubbery region), the polymer–filler, filler–filler, and filler–aggregate interactions can bring more pronounced effect on

the storage modulus value due to larger deviations between the underlying thermodynamics of these materials.[1,2,35] The high temperature behavior is much more affected by the strength of interphase interactions between all the components presenct in the EVA nanocomposites. In agreement with TGA analysis, the significant loss of EVA mechanical integrity at high temperature condition upon the MMT (W) inclusion can be attributed by the reduction of interphase bonding between the PVA and PE monomers and weaker interfacial interactions between the organo-MMT-EVA due to poorer quality of organo-MMT dispersion and exfoliation (as observed in TEM and XRD).

In contrast, when the EVA was added with 5MMT (T), the storage modulus was increased significantly throughout the applied heating range with a simultaneous decrease in intensity and broadening of the relaxation peak (Figure 10). This might be attributed by the quality of organo-MMT dispersion and exfoliation in the EVA that were found better when toluene was used as the pre-dispersing medium (Figures 4 and 5). The presence of greater number of the exfoliated organo-MMT structure in the EVA resulted in its more restricted molecular mobility, thus higher modulus was achieved.

Figure 12 presents the tan δ versus temperature curves of neat EVA and EVA nanocomposites containing water and toluene dispersed organo-MMTs. The EVA resin used in this study is a random copolymer that exhibit intermediate properties between the two homopolymers; polyethylene and poly(vinyl acetate). The properties of this material are dependent on the proportion and interaction of both co-monomers. Due to this factor, the EVA thermal transition and relaxation processes are known to be quite complex.[30,35] According to Yamaki *et al.*,[36] the EVA copolymer structure possesses microheterogeneous distribution of the molecules in a polymer host. Some of the molecules might be located near the VAc domains and others near the ethylene blocks of the copolymers. Obviously, the damping behavior of both EVA_5MMT (T) and EVA_5MMT (W) presents a great example of this situation. At the same temperature region, the neat EVA and EVA containing toluene dispersed organo-MMT exhibit similar tan δ curve, where one well defined damping peak was observed. According to Arsac *et al.*, this transition peak in the range of 35–50°C corresponds to the softening temperature for poly(vinyl acetate) (T_1).[31] When the EVA was added with 5 wt % MMT (T), this transition peak was shifted to slightly higher temperature with a broader peak, which indicates more restricted molecular mobility imposed by the dispersed organo-MMT in the EVA molecular chains.

An anomalous behavior was observed when the EVA was added with water dispersed organo-MMT. The broadening of this T_1 peak can be observed, while the presence of another diffuse and broad peak centered at ~60°C (T_2) can be seen. The transition occurred in the range of 57–67°C can be related to the onset of the melting point of the EVA copolymers.[36] In copolymer, where both polar and non-polar components exist, an interruption of longer sequences of identical groups with molecular structures of different polarity or geometry can lead to nanophase separation.[37] Therefore, at an elevated temperature, the dynamic force applied and the accumulation of the hydrophobic and long surfactant chains at the interfaces of the ethylene monomers was anticipated to lead in disordering, decoupled chain segments, and phase separation of PE/PVA. As a result, shorter PVA chains were produced and broader T1 peak appeared. The melting of the PE crystals also would occur at lower temperature due to the above mentioned factors. Therefore, EVA_5MMT (W) nanocomposite exhibits lower melting temperature than neat EVA and EVA_5MMT (T). Based on DMTA scan, the melting temperature of the EVA_5MMT (W) was found to be at ~60°C (T_2), while for EVA and EVA_5MMT (T), the melting point was beyond the measurement temperature (> 80°C). These T1 and T2 transitions have been confirmed through the DSC analysis, which will be discussed in the following section. The lowest thermal stability of the EVA_5MMT (W) sample is in good agreement with TGA results where EVA_5MMT (W) possesses the lowest degradation peak temperatures during the first and second step mass loss as compared to other materials.

Differential Scanning Calorimetry

DSC analysis was performed to further investigate the thermal behavior of neat EVA and EVA nanocomposites and the DSC heating scans are presented in Figure 13. In agreement with the findings of Stark and Jaunich,[38] we observe two endotherms and they have been labeled T1 and T2. A less intense T1 endotherm centered at ~50°C corresponds to the softening temperature of PVA.[31] This is also a reflection of T1 transition observed through the DMTA. When benchmarked with the host EVA, more prominent softening transition can be seen in the EVA_5MMT (T), while weaker softening transition and slightly lower T1 peak can be observed in the EVA_5MMT (W) material. The stronger T1 signal in the EVA_5MMT (T) could probably due to favorable EVA–nanofiller interactions, which require greater heat energy for molecular motions. As mentioned earlier, lower T1 signal in EVA_5MMT (W) can be associated with the disruption of chain order and inhomogeneity of PVA distribution in the EVA_5MMT (W) nanocomposite structure. A T2 endotherm, which is more intense than T1 endotherm appears in the temperature range of 60°C to 100°C. The T2 peak was observed around 90°C and can be related to the melting point of the EVA copolymer.[31,38] However, the onset melting temperatures of the EVA and EVA nanocomposites are difficult to discern from the DSC scans due to this broad melting range.

It is known that the melting endotherm of the EVA copolymer is attributed to the melting of polyethylene crystallites.[31,38] The degree of crystallinity can be induced by the nanofiller incorporation. It is apparent from the DSC curves that the melting peak (T2) of host EVA is the sharpest among the three materials, suggesting that the host material has more ordered PE crystallite structure. In agreement with the XRD results, the broader T2 endotherms of both EVA nanocomposites suggests that the crystallinity of the PE has been reduced due to the incorporation of the pre-dispersed organo-MMTs. Fewer and shorter PE segments being crystallized as they were more likely to interact with the organo-MMT nanofiller. It is also noticeable that the

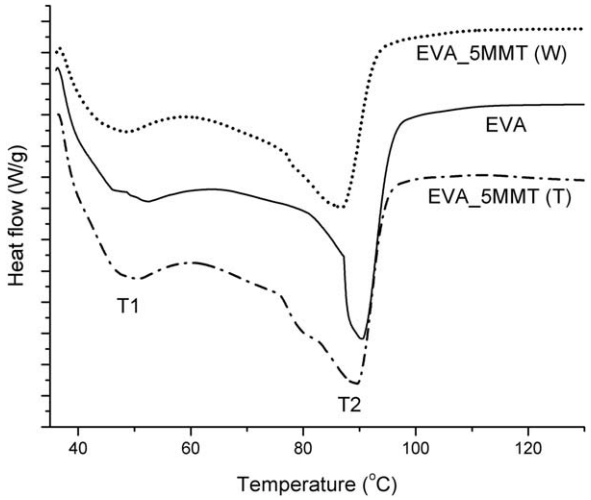

Figure 13. DSC heating curves for neat EVA, EVA_5MMT (W) and EVA_5MMT (T) nanocomposites.

T2 of the EVA_5MMT (W) is ~4°C lower than the EVA and EVA_5MMT (T). In line with the previous TGA and DMTA results, this was possibly due to weaker PE-PVA interphase bonding.

Based on the TEM, XRD, FTIR, TGA and DMTA, and DSC data, the schematic structure of the organo-MMT and the melt compounded EVA nanocomposites containing the pre-dispersed organo-MMT can be postulated and illustrated in Figure 14. The pre-dispersing process using water medium might cause the avoidance of the surfactant's hydrophobic tails from the hydrophilic environment, resulting in their precipitation in the medium. This might prevent the entrance of greater amounts of water molecules into the organo-MMT inter-galleries in order to destabilize the binding energy within the inter-galleries. Consequently, this could hinder larger degree of tactoid loosening during the pre-dispersing process. Due to their long segment and restricted mobility, there is also high possibility that most of the surfactant chains retain its organization and distribution in the MMT, even when the water dried off. When the MMT (W) is added to the EVA matrix, the inhomogeneous surfactant distribution leads to the inhomogeneous PE and PVA distribution in the host copolymer too. This is due to the affinity of the precipitated long surfactant's tails toward the hydrophobic PE chains, rather than hydrophilic PVA chains. As a result, weaker nanofiller–polymer interactions and hence poorer quality of nanofiller dispersion were obtained. Certainly, these would not occur when hydrophobic pre-dispersing medium (toluene) was used, as the hydrophobic surfactant would not repel toluene from entering the inter-galleries. More homogeneous distribution of the surfactant, PVA, PE, was obtained. As a result, the incorporation of MMT (T) into the EVA host polymer caused greater EVA-organo-MMT interactions, and hence higher degree of exfoliation and dispersion as compared to MMT (W). Apparently, the obtained greater tensile properties of EVA containing the 5MMT (T) as compared to the 5MMT (W) could also be related with this morphology.

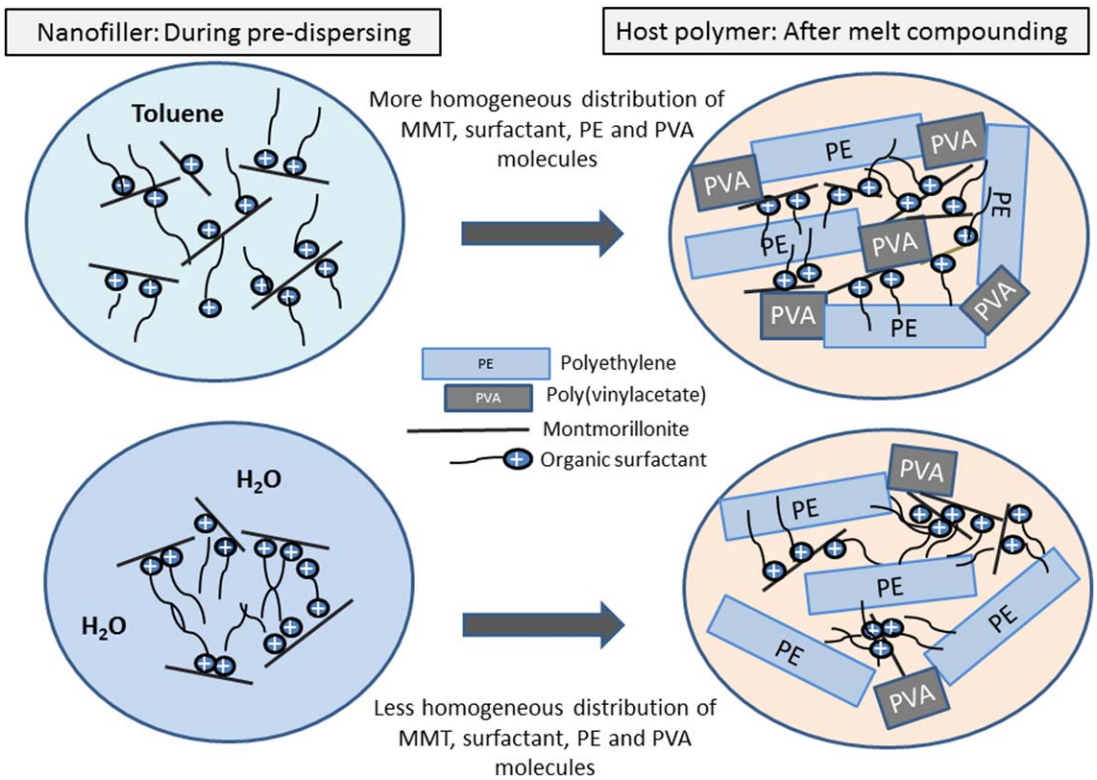

Figure 14. The morphology of the organo-MMT nanofillers during the pre-dispersing process and their respective melt compounded EVA nanocomposites. [Color figure can be viewed in the online issue, which is available at wileyonlinelibrary.com.]

CONCLUSION

The effects of organo-MMT nanofiller loading and pre-dispersing medium on the morphology, mechanical and thermal properties of neat EVA and EVA nanocomposites were studied. TEM and XRD analyses revealed that the pre-dispersing medium and concentration of the organo-MMT nanofiller gave significant effect on its exfoliation and dispersion characteristic in the EVA host polymer. The pre-dispersing technique using water has resulted in improved quality of the organo-MMT exfoliation and dispersion as compared to the non-pre-dispersed organo-MMT/EVA nanocomposite system, reported in previous publication. However, a greater degree of organo-MMT exfoliation and dispersion was obtained when toluene was used as medium to replace water. These suggest that the pre-dispersing technique done prior to melt compounding of the organo-MMT and EVA can assist in greater nanofiller exfoliation and dispersion efficiency, thus improve the quality of the produced EVA nanocomposites. Overall, the tensile properties of the EVA nanocomposites containing toluene dispersed organo-MMT were higher than that of water dispersed organo-MMT. This can be related with the morphology of the EVA nanocomposite system containing toluene dispersed organo-MMT that exhibit greater nanofiller exfoliation and dispersion as compared to water dispersed organo-MMT counterparts. Of particular interest, the increase of filler loading from 0 to 5 wt % has resulted in markedly improved EVA tensile strength and toughness. Comparing the results of DMTA and DSC of host EVA and EVA nanocomposites lead us to postulate that the addition of the pre-dispersed organo-MMT can give significant effect on the strength of interphase interaction between the different polarity monomers presence in this copolymer structure and subsequent thermal transition of this copolymer. Based on TGA results, the thermal stability of the EVA was improved with the addition of 5 wt % organo-MMT pre-dispersed by toluene. In contrary, the incorporation of 5 wt % organo-MMT pre-dispersed by water resulted in the reduction of thermal stability of the EVA. This can be related with more severe weakening effect to the interphase bonding between the PE and PVA components in the EVA when subjected to high temperature condition.

ACKNOWLEDGMENTS

This research was funded by Fundamental Research Grant Scheme (FRGS) (9003-00473) from the Ministry of Higher Education, Malaysia. The authors thank Assoc. Prof Dr Salmah Husseinsyah for lending her experimental apparatus during this research and School of Environmental Engineering, UniMAP for FTIR analysis.

AUTHOR CONTRIBUTIONS

The manuscript was written through contributions of all authors as per following: Azlin Fazlina Osman: Designed experiments, Wrote the paper, Analysis and interpretation of data; Hussein Kalo: Assisted with XRD and TEM experiments and analyses, Critical review of the paper; Mohd Saifullah Hassan: Processing and preparation of the samples, Mechanical tests and analyses; Tew Wei Hong: Processing and preparation of the samples, Mechanical tests and analyses; Farehah Azmi: Assisted with thermal tests and FTIR analyses, Edited paper. All authors have given approval to the final version and submission.

REFERENCES

1. Osman, A. F.; Edwards, G. A.; Schiller, T. L.; Andriani, Y.; Jack, K. S.; Morrow, I. C.; Halley, P. J.; Martin, D. J. *Macromolecules* **2012**, *45*, 198.
2. Osman, A. F.; Andriani, Y.; Edwards, G. A.; Schiller, T. L.; Jack, K. S.; Morrow, I. C.; Halley, P. J.; Martin, D. J. *RSC Adv.* **2012**, *2*, 9151.
3. Kalendova, A.; Merinska, D.; Gerard, J. F.; Slouf, M. *Polym. Compos.* **2013**, *34*, 1418.
4. Andriani, Y.; Morrow, I. C.; Taran, E.; Edwards, G. A.; Schiller, T. L.; Osman, A. F.; Martin, D. *J. Acta Biomater.* **2013**, *9*, 8308.
5. Osman, A. F.; Alakrach, A.; Kalo, H.; Dahham, O. S.; Abdullah, M. A. B. *Appl. Mech. Mater.* **2015**, *754*, 24.
6. Osman, A. F.; Alakrach, A. M.; Kalo, H.; Azmi, W. N. W.; Hashim, F. *RSC Adv.* **2015**, *5*, 31485.
7. Carvalho, H. W.; Santilli, C. V.; Briois, V.; Pulcinelli, S. H. *RSC Adv.* **2013**, *3*, 22830.
8. Leszczyńska, A.; Njuguna, J.; Pielichowski, K.; Banerjee, J. R. *Thermochim. Acta* **2007**, *454*, 1.
9. Kiliaris, P.; Papaspyrides, C. D. *Prog. Polym. Sci.* **2010**, *35*, 902.
10. Wang, S.; Hu, Y.; Zong, R.; Tang, Y.; Chen, Z.; Fan, W. *Appl. Clay Sci.* **2004**, *25*, 49.
11. Pavlidou, S.; Papaspyrides, C. D. *Prog. Polym. Sci.* **2008**, *33*, 1119.
12. Kango, S.; Kalia, S.; Celli, A.; Njuguna, J.; Habibi, Y.; Kumar, R. *Prog. Polym. Sci.* **2013**, *38*, 1232.
13. Jones, T. R. *Clay Miner.* **1983**, *18*, 399.
14. Pereira, K. R. D. O.; Hanna, R. A.; Vianna, M. M. G. R.; Pinto, C. A.; Rodrigues, M. G. F.; Valenzuela-Diaz, F. R. *Mater. Res.* **2005**, *8*, 77.
15. Volzone, C.; Rinaldi, J. O.; Ortiga, J. *Mater. Res.* **2000**, *3*, 115.
16. Fink, J. K. Ethylene vinyl acetate copolymers. In Handbook of Engineering and Specialty Thermoplastics. Volume *1*: Polyolefins and Styrenics; Couper, J. E. R.; Islam, R.; Lieberman, N.; Muhlbauer, W. K.; Sherif, S. A.; Erdlac, R.; Khaladkar, P.; Martin, P.; Nee, A. Y. C.; Speight, J. G., Eds.; Wiley: Hoboken, NJ, USA, **2010**; p 187.
17. Peacock, A. J. Handbook of Polyethylene: Structures, Properties, and Applications; CRC Press: New York, USA, **2000**.
18. Atkin, R.; Craig, V. S. J.; Wanless, E. J.; Biggs, S. *Adv. Colloid Interface Sci.* **2003**, *103*, 219.
19. Hanley, H. J. M.; Muzny, C. D.; Ho, D. L.; Glinka, C. *J. Langmuir* **2003**, *19*, 5575.
20. Andriani, Y.; Jack, K. S.; Gilbert, E. P.; Edwards, G. A.; Schiller, T. L.; Strounina, E.; Osman, A. F.; Martin, D. J. *J. Colloid Interface Sci.* **2013**, *409*, 72.

21. Mollet, V. A.; Kamal, M. R. *J. Polym. Eng.* **2006**, *26*, 757.
22. Elisabetta, U.; Gaetano, G.; Michele, M. *Soft Nanosci. Lett.* **2011**, *1*, 105.
23. Merinska, D.; Kalendova, A.; Dujkova, Z.; Slouf, M.; & Simonik, J. In Proceedings of the 4th WSEAS International Conference on Biochemistry and Medical Chemistry (BIO-MEDCH'13), WSEAS Press: Athens, Greece, **2013**; p 35.
24. Bishop, J. L.; Pieters, C. M.; Edwards, J. O. *Clays Clay Miner.* **1994**, *42*, 702.
25. Arroyo, M.; Lopez-Manchado, M. A.; Herrero, B. *Polymer* **2003**, *44*, 2447.
26. Alshabanat, M.; Al-Arrash, A.; Mekhamer, W. *J. Nanomater.* **2013**, *9*, 1.
27. Workman, J., Jr.; Weyer, L. Practical Guide to Interpretive Near-Infrared Spectroscopy; CRC press: New York, USA, **2007**; p 71.
28. Jamroz, N. U. *J. Chem. Soe. Pak.* **2003**, *25*, 84.
29. Wilson, R.; George, S. M.; Maria, H. J.; Plivelic, T. S.; Kumar, S. A.; Thomas, S. *J. Phys. Chem. C* **2012**, *116*, 20002.
30. Leszczyńska, A.; Njuguna, J.; Pielichowski, K.; Banerjee, J. R. *Thermochim. Acta* **2007**, *453*, 75.
31. Arsac, A.; Carrot, C.; Guillet, J. *J. Therm. Anal. Calorim.* **2000**, *61*, 681.
32. Ray, S. S.; Okamoto, M. *Prog. Polym. Sci.* **2003**, *28*, 1539.
33. Corcione, C. E.; Greco, A.; Frigione, M.; Maffezzoli, A. In: Polymer Composites; Thomas, S.; Joseph, K; Malhotra, S. K.; Goda, K.; Sreekala, M. S., Eds.; Wiley-CVH Verlag GmbH & Co. KGaA: Weinheim, Germany, **2013**; Vol. *2*, p 201.
34. Alosime, E. M.; Edwards, G. A.; Martin, D. J. *J Appl. Polym. Sci.* **2015**, *132*, 41742.
35. Osman, A. F.; Halley, P.; Martin, D. *Adv. Mater. Res.* **2013**, *795*, 9.
36. Yamaki, S. B.; Prado, E. A.; Atvars, T. D. Z. *Eur. Polym. J.* **2002**, *38*, 1811.
37. Wunderlich, B. Thermal Analysis of Polymeric Materials; Springer Science & Business Media: Heidelberg, Germany, **2005**; p 757.
38. Stark, W.; Jaunich, M. *Polymer Testing* **2011**, *30*, 236.